

J. G. Gonzalez-Rodriguez · M. Casales
V. M. Salinas-Bravo · M. A. Espinosa-Medina
A. Martinez-Villafañe

Electrochemical noise generated during the stress corrosion cracking of sensitized alloy 690

Received: 3 December 2002 / Accepted: 25 August 2003 / Published online: 31 October 2003
© Springer-Verlag 2003

Abstract Electrochemical noise in current has been used to monitor the stress corrosion cracking (SCC) susceptibility of alloy 690 sensitized at 700 °C during 48 h in sodium thiosulfate at 90 °C. At 48 h of aging, the specimen failed by SCC and the corrosion current pulses had high intensity and low frequency, and were associated with the nucleation and propagation of stress corrosion cracks during slow strain rate tests. When the alloy was immune to SCC, the observed corrosion current pulses had a much higher frequency and lower intensity, indicating either uniform corrosion or passivation. The type of transients observed do not indicate the mechanism responsible for the observed embrittlement, but only the cracking initiation or propagation process.

Keywords Alloy 690 · Electrochemical noise · Stress corrosion cracking

Introduction

Electrochemical noise has been successfully applied to the study of passivation, uniform corrosion and pitting corrosion of aluminum in deionized water, in 0.1 wt% NaOH and 302-type stainless steel in 3.5% NaCl [1], not only for the corrosion rate, but also for the type of corrosion, especially for pitting studies [2, 3, 4, 5, 6, 7, 8, 9]. However, the use of electrochemical noise for the study of stress corrosion cracking (SCC) has been limited. Newman and Sieradzki [10] used the random fluctuations in current during the transgranular SCC of α -brass in sodium nitrite to demonstrate the discontinuous nature of cracking in this system. Loto and Cottis [11] made an investigation of the electrochemical noise (voltage) generated during the SCC of α -brass in Mattson solution, analyzing the readings with the maximum entropy method. They found that the measured parameters which appeared to give the clearest indication of the results were the standard deviation and the roll-off slope, finding also that the cracking of the specimens gave the highest noise amplitudes in most cases as well as the highest standard deviation peaks. They also did similar studies for an aluminum alloy in 3.5% NaCl solution [12] and for a high-strength carbon steel in 3.5% NaCl + 500 ppm Na₂S [13], finding similar results to those found for α -brass, with the difference that the data for carbon steel were analyzed with both the maximum entropy method and with fast Fourier transform. The Harwell group has done excellent work on the intergranular SCC of sensitized type 304 stainless steel in dilute thiosulfate solutions at both room and high temperatures [14, 15], using the slow strain rate testing technique. They found that, in both cases, corrosion current pulses were associated with the nucleation of microcracks and their movement across a few grain boundary facets. More recently, Gonzalez-Rodriguez and co-workers [16, 17] related the corrosion potential fluctuations with the nucleation and growth of stress corrosion cracks in 17-4PH and 410 stainless steels in NaCl solutions.

J. G. Gonzalez-Rodriguez (✉)
CIICAp, UAEM, Av. Universidad 1001,
62210 Cuernavaca, Mor., Mexico
E-mail: ggonzalez@uaem.mx

M. Casales
Centro de Ciencias Físicas,
UNAM, Av. Universidad S/N,
Cuernavaca, Mor., Mexico

V. M. Salinas-Bravo
Instituto de Inv. Electricas,
Av. Reforma 118, Temixco,
Mor., Mexico

M. A. Espinosa-Medina
IMP, Eje Central Lazaro Cardenas 108,
D.F., Mexico

A. Martinez-Villafañe
CIMAV,
Complejo Industrial Chihuahua,
Chihuahua, Mexico

The present work is concerned with the electrochemical noise measurements obtained during the SCC of sensitized alloy 690, a material used for heat exchanger tubes in the nuclear power industry and which is more resistant to SCC than the normally used alloy 600.

Experimental

The commercially produced alloy 690 used was in the form of a mill-annealed tube, 11 mm thick and 50.8 mm inner diameter. Its chemical composition was (wt%) Ni-32.3Cr-6.8Fe-0.34Al-0.30Si-0.15Mn-0.23-0.06C. The specimens were solution annealed at 1100 °C for 30 min and water quenched. After this, the specimens were sensitized at 700 °C for 5, 12, 24, 36, 48 and 72 h and then water quenched. SCC was performed in 0.01 M Na₂S₂O₃ at 90 °C and in air under deformation conditions at a strain rate of $1.0 \times 10^{-6} \text{ s}^{-1}$ by slow strain rate testing. Cylindrical tensile specimens having a gauge diameter of 2.5 mm and 25 mm in length were machined from the tube. All the solutions were prepared using analytical grade reagents. All the tests were performed at the free corrosion potential. The measurements were made with a zero resistance ammeter, from ACM Instruments, controlled with a desktop computer, which also served to record the readings on floppy disks. Time records consisted of blocks of 1024 readings, taken at 1 s intervals, using a two-electrodes arrangement, the tensile specimen and another portion taken from another tensile specimen from the same tube, under the same heat treatment but previously fractured in air. The annealing and sensitization treatments were performed under the machined tensile specimens. Only the area of the gauge section was exposed to the electrolyte; the rest of the specimen was masked with a special resin. Other than the delay in storing the data on the floppy disk, time records were taken continuously throughout the test. To measure the degree of sensitization (DOS), the double loop electrochemical potentiodynamic reactivation (DL-EPR) test in 0.5 M H₂SO₄ + 0.0001 M KCNS (potassium thiocyanate) at a sweep rate of 60 mV/min was used. The polarization curves started from the cathodic side and went towards the anodic direction. The electrochemical potential of the specimens was measured with respect to a saturated calomel electrode (SCE) with graphite as the counter electrode. The current ratio (CR) was used as the parameter to measure the DOS of the steel according to:

$$\%CR = 100(I_r/I_a) \quad (1)$$

where I_a is the critical current before the passive region is reached when going in the anodic direction, and I_r is the critical current reached in the reverse scanning, as shown in Fig. 1. These experiments were performed twice, whereas the slow strain rate tests were performed only once, but the electrochemical noise measurements were taken throughout these experiments every 17 min during around 28 h, depending of the time duration of the experiment.

Results

Table 1 shows the results of the DL-EPR tests on the aged samples of alloy 690. It can be seen that the I_a/I_r value decreases from the mill annealing condition to the specimen aged for 5 h, and then it increases until reaching its maximum value in the specimen aged for 48 h, indicating that this specimen was the most susceptible to SCC. After this, the DOS decreases again for the specimen aged for 72 h. According to the depleted zone theory, the self-healing (or desensitization) results from the diffusion of chromium into the depleted zone

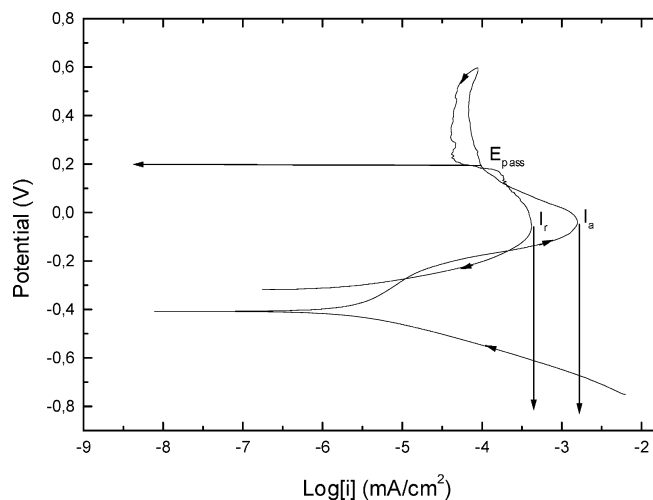


Fig. 1 Typical potentiodynamic curve of sensitized alloy 690 as measured in the DL-EPR test solution

from the matrix further away from the grain boundaries. Baumele [18] suggested that grain boundary diffusion of chromium is responsible for sensitization and that volume diffusion of chromium was associated with self-healing. In fact, both processes occur, but diffusion along grain boundaries is faster than in the matrix. The chromium content in the grain boundaries is low even between intergranular carbides, but the chromium depletion profile occurs because of chromium diffusion in the matrix near the grain boundaries.

Figure 2 shows the current transients in the elastic zone, the yielding point and the ultimate tensile strength (UTS) points for the as-received specimen of its stress-deformation curve. At the elastic point, the current fluctuations are anodic, of very high frequency and low intensity, indicating uniform corrosion, but at the yielding point there are some anodic current fluctuations of much smaller frequency and higher intensity. These types of fluctuations continue, appearing up to the UTS. It must be clarified that since the fluctuations were taken every 1024 s, around 17 min, continuously throughout the tensile experiments, only the more representative time series are shown here, because they had a very high reproducibility.

Current fluctuations at the yielding point for specimens aged during 5, 12, 24, 36 and 72 h are shown in Fig. 3. It can be seen that for the specimen sensitized

Table 1 Results of the DL-EPR tests for alloy 690 sensitized at different times

Sensitization time (h)	$I_r/I_a \times 100$
As-received (mill-annealed)	13
5	1
12	2
24	5
36	20
48	32
72	12

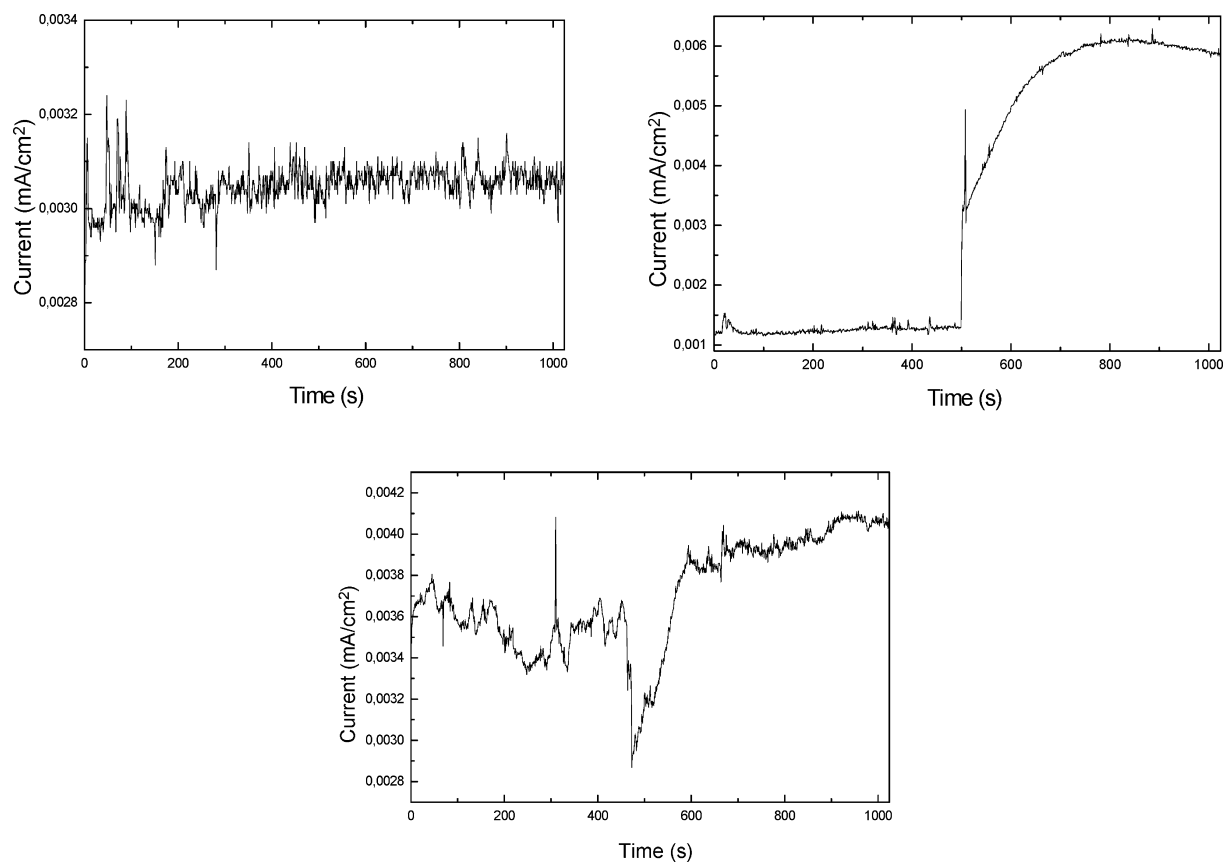


Fig. 2 Current fluctuations at (*top left*) the elastic zone, (*top right*) the yielding point and (*bottom*) the ultimate tensile strength, for the as-received alloy 690

during 5 h, transients of very high frequency are observed, characteristic of uniform corrosion. At 12 h of aging there start to appear some transients where the current shows a sudden increase, but after it tends to recover, in a slow fashion, its original value. At 24 h and 36 h of aging, this is more evident. At 72 h of aging, where the specimen did not fail by SCC, the current fluctuations were of lower frequency and intensity than those observed at 5, 12, 24 and 36 h of aging.

The time series for specimens sensitized during 48 h are shown in Fig. 4. Some anodic (i.e. positive going) transients of very low frequency, but higher intensity, can be observed. When the large transients recover their original value, these high-frequency transients overlap the small transients. This specimen failed by intergranular SCC and it was shown previously [19] that the cracking was due to anodic dissolution, so these transients are related to crack initiation and propagation processes.

Figure 5 shows the fast Fourier transform (FFT) of the time series shown in Figs. 2, 3, 4. It can be seen that the intensity of the FFT curve for the specimen which failed by SCC, i.e. the one aged for 48 h, is higher than that obtained for specimens which did not fail by SCC, i.e. those specimens aged during shorter or longer times than 48 h.

Discussion

When the specimen failed by SCC, the transients observed were anodic (positive going), but if the specimen did not fail by stress corrosion cracking, the transients observed had a lower intensity and a much higher frequency. It is considered that these transients are the result of a film rupture which exposes metal to the solution. The current transient is the result of exposure of the anode and their relatively slow current recovery reflects, perhaps, a repassivation process. The transient ceases on reformation of the film. The anodic transients observed during SCC suggest that these events are associated with an electron consuming reaction (cathodic discharge of the specimen). Once the crack initiated, the crack propagation process was followed by the reduction of water to hydrogen atoms and hydroxyl ions at the crack tip. If the specimen did not fail by SCC, then the transients observed must be related to the pitting corrosion process. Eden et al. [20] also found cathodic transients of low intensity during the pitting corrosion of type 304 stainless steel. It is considered that these transients are the result of a film rupture which exposes metal to the solution. The transients are the result of exposure of the anodic area, which is accompanied by the discharge of the electrochemical double layer by the electrons produced by the metal dissolution reaction. The relatively slow potential recovery, according to the authors, is the recharging of the double layer by the

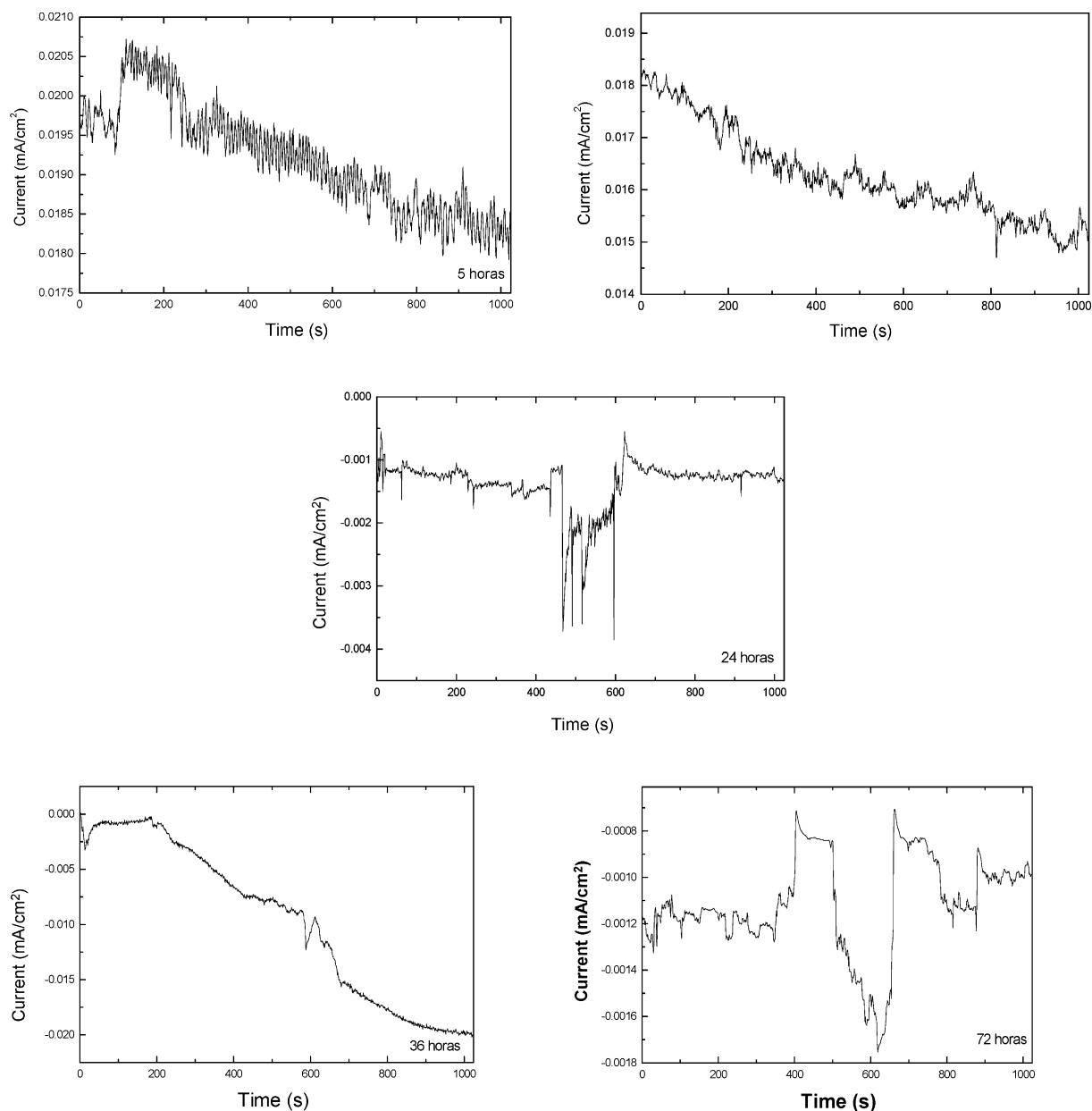


Fig. 3 Current fluctuations at the yielding point for alloy 690 aged during (top left) 5 h, (top right) 12 h, (middle) 24 h, (bottom left) 36 h and (bottom right) 72 h

cathodic reduction reaction, but we think this is due to a repassivation process. The drop in potential ceases on reformation of the film.

The anodic transients observed during SCC suggest that these events are associated with an electron consuming reaction, i.e. cathodic discharge of the specimen. The first events could have been the result of a film rupture process, and probably this is the reason why, before yielding, a lot of small amplitude transients were observed. Once the crack initiated, the crack propagation process was followed by the reduction of water to hydrogen atoms and hydroxyl ions at the crack tip. In previous work [19] it was shown that, even under anodic

polarization, the cracking mechanism in this system was one of hydrogen embrittlement. In the cases where the specimen did not fail by SCC but it was not pitted either, a white noise pattern, which consisted of random signal fluctuations, was observed, which means that the specimen is undergoing uniform corrosion [17]. The transients observed in this case are probably due to the exposure of fresh metal to the environment once necking has initiated, allowing anodic dissolution of the metal. In fact, Eden et al. [20] found that the transients observed during the transgranular SCC of carbon steel in a CO/CO₂ mixture were similar to those found in this work; they were, however, of very low intensity. However, in the present work, the steel showed intergranular features. On the other hand, the transients observed during the intergranular SCC of a 304 stainless steel exposed to chloride ions were anodic, followed imme-

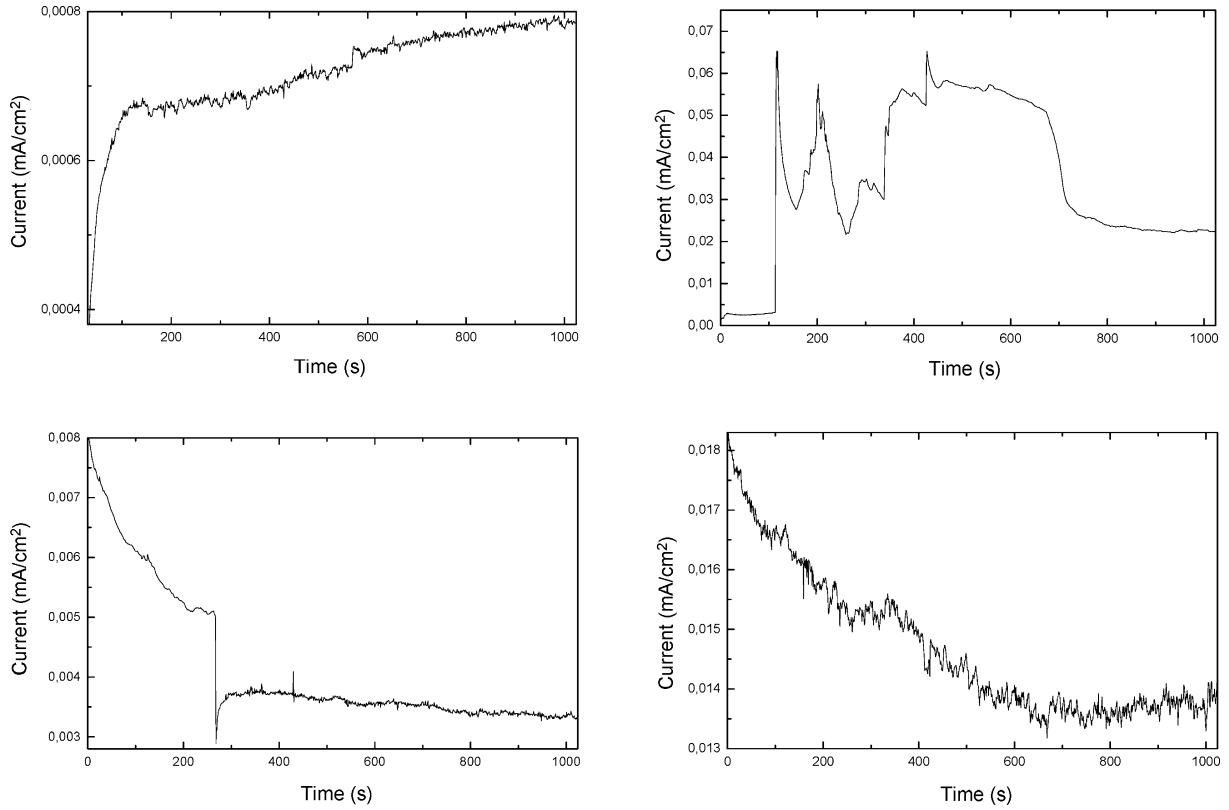


Fig. 4 Current fluctuations at (*top left*) the elastic zone, (*top right*) the yielding point, (*bottom left*) the ultimate tensile strength and (*bottom right*) the final fracture for alloy 690 aged during 48 h

diately by a cathodic peak, and afterwards the recovery of the original value. For the case of the carbon steel, Eden et al. [20] argued a hydrogen embrittlement mechanism, like in the present work, whereas for the case of the stainless steel the mechanism was not too obvious. These results suggest that the type of transients observed do not indicate the mechanism responsible for the observed embrittlement, but only the cracking initiation or propagation process. Two different cracking mechanisms can give similar transients and, conversely, the same mechanism can give different types of transients, depending of the material/environment combination. The most important fact is that electrochemical noise is a very powerful technique to detect the initiation and propagation of stress corrosion cracks.

Conclusions

When the alloy 690 specimen failed by SCC, the corrosion current pulses had a low frequency and high intensity. They were associated with the nucleation and propagation of stress corrosion cracks in 0.01 M Na₂S₂O₃ at 90 °C during slow strain rate tests. When it

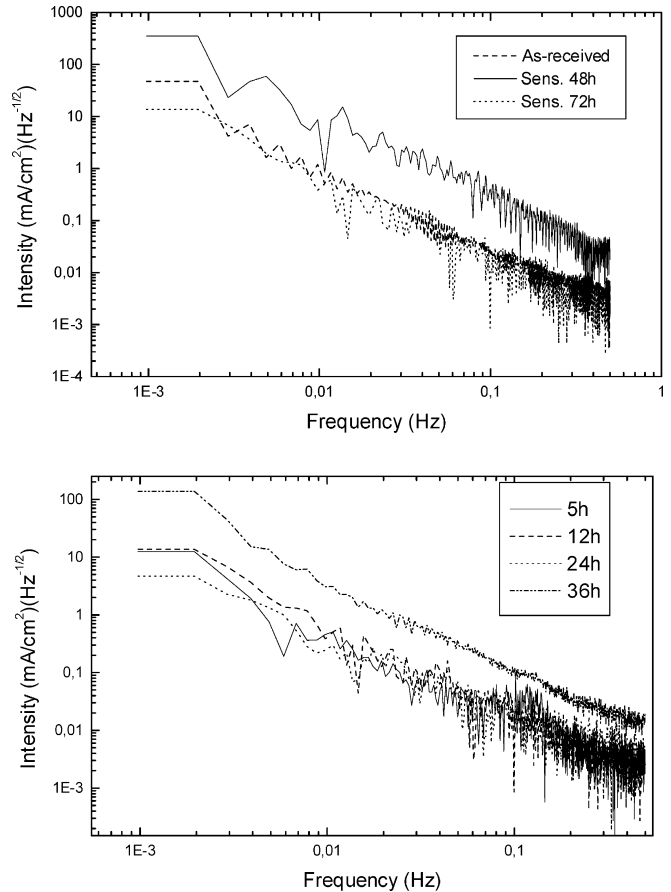


Fig. 5 Fast Fourier transform of specimens (*top*) as-received and aged for 48 and 72 h, and (*bottom*) aged during 5, 12, 24 and 36 h

was immune to SCC, the current transients had a much higher frequency and lower intensity, and they indicated either passivation or uniform corrosion. The types of transients observed do not indicate the mechanism responsible for the observed embrittlement, but only the cracking initiation or propagation process.

References

1. Legat A, Dolecek V (1995) *Corrosion* 51:295
2. Mansfield F, Xiao H (1993) *J Electrochem Soc* 140:2205
3. Sherrat M, Robinson FPA, Tullmin M, Rothwell AN (1994) *Br Corros J* 129:33
4. Shibata T, Orikawa J, Fujimoto S (1989) *Corros Eng* 38:175
5. Hdlaky K, Dawson JL (1981) *Corros Sci* 21:317
6. Hdlaky K, Dawson JL (1982) *Corros Sci* 22:231
7. Gabrielli C, Huet F, Keddam M (1986) *Electrochim Acta* 31:1025
8. Uruchurto-Chavarin J (1991) *Corrosion* 47:472
9. Williams DE, Wescott C, Fleischmann M (1984) *J Electroanal Chem* 180:549
10. Newman RC, Sieradzki K (1983) *Scr Met* 17:621
11. Loto CA, Cottis RA (1987) *Corrosion* 43:499
12. Loto CA, Cottis RA (1989) *Corrosion* 45:136
13. Cottis RA, Loto CA (1990) *Corrosion* 46:12
14. Wells DB, Stewart J, Davison R, Scott PM, Williams DE (1992) *Corros Sci* 33:39
15. Stewart J, Wells DB, Scott PM, Williams DE (1992) *Corros Sci* 33:73
16. Gonzalez-Rodriguez JG, Salinas-Bravo VM, Garcia-Ochoa E, Diaz-Sanchez A (1997) *Corrosion* 53:693
17. Casales M, Espinoza MA, Martinez-Villafañe A, Salinas-Bravo VM, Gonzalez-Rodriguez JG (2000) *Corrosion* 56:1133
18. Baumel A (1964) *Corros Sci* 4:89
19. Casales M, Martinez-Villafañe A, Salinas-Bravo VM, Gonzalez-Rodriguez JG (2002) *Mater Sci Eng A* 332:223
20. Eden DA, Rothwell AN, Dawson JL (1991) Presented at *Corrosion '91*, Houston, Tex., paper 44